



Published in final edited form as:

Neuroscience. 2013 January 15; 229: 77–87. doi:10.1016/j.neuroscience.2012.10.066.

Cervical spinal demyelination with ethidium bromide impairs respiratory (phrenic) activity and forelimb motor behavior in rats

Nicole L. Nichols^a, Antonio M. Punzo^b, Ian D. Duncan^c, Gordon S. Mitchell^a, and Rebecca A. Johnson^b

^aDepartment of Comparative Biosciences, University of Wisconsin, Madison, WI 53706

^bDepartment of Surgical Sciences, University of Wisconsin, Madison, WI 53706

^cDepartment of Medical Sciences, University of Wisconsin, Madison, WI 53706

Abstract

Although respiratory complications are a major cause of morbidity/mortality in many neural injuries or diseases, little is known concerning mechanisms whereby deficient myelin impairs breathing, or how patients compensate for such changes. Here, we tested the hypothesis that respiratory and forelimb motor function are impaired in a rat model of focal dorsolateral spinal demyelination (ethidium bromide, EB). Ventilation, phrenic nerve activity and horizontal ladder walking were performed 7–14 days post-C₂ injection of EB or vehicle (SHAM). EB caused dorsolateral demyelination at C₂–C₃ followed by significant spontaneous remyelination at 14 days post-EB. Although ventilation did not differ between groups, ipsilateral integrated phrenic nerve burst amplitude was significantly reduced versus SHAM during chemoreceptor activation at 7 days post-EB but recovered by 14 days. The ratio of ipsi- to contralateral phrenic nerve amplitude correlated with cross-sectional lesion area. This ratio was significantly reduced 7 days post-EB versus SHAM during baseline conditions, and versus SHAM and 14 day groups during chemoreceptor activation. Limb function ipsilateral to EB was impaired 7 days post-EB and partially recovered by 14 days post-EB. EB provides a reversible model of focal, spinal demyelination, and may be a useful model to study mechanisms of functional impairment and recovery via motor plasticity, or the efficacy of new therapeutic interventions to reduce severity or duration of disease.

© 2012 IBRO. Published by Elsevier Ltd. All rights reserved.

Corresponding author: Rebecca A. Johnson Assistant Clinical Professor Dept. of Surgical Sciences University of Wisconsin 2015 Linden Drive Madison, WI 53706 Phone: (608) 265-5485 FAX: (608) 263-7930 pipob@svm.vetmed.wisc.edu. nichols.36@wright.eduduncani@svm.vetmed.wisc.eduahayes3@svm.vetmed.wisc.edumitchell@svm.vetmed.wisc.edu.

Publisher's Disclaimer: This is a PDF file of an unedited manuscript that has been accepted for publication. As a service to our customers we are providing this early version of the manuscript. The manuscript will undergo copyediting, typesetting, and review of the resulting proof before it is published in its final citable form. Please note that during the production process errors may be discovered which could affect the content, and all legal disclaimers that apply to the journal pertain.

AUTHOR CONTRIBUTIONS

Nicole L. Nichols collected and analyzed neurophysiological data and edited the manuscript.

Antonio M. Punzo collected and analyzed breathing, forelimb function, and tissue lesion data.

Ian D. Duncan advised on lesion creation, analyzed anatomical data, and edited the manuscript.

Gordon S. Mitchell designed breathing experiments, consulted on the respiratory and forelimb data interpretation and edited the manuscript.

Rebecca A. Johnson initiated the project, designed breathing and forelimb function experiments, analyzed and interpreted respiratory and forelimb function data, and prepared the manuscript.

DISCLOSURES: There are no known conflicts of interest.

Keywords

motor function; compensatory plasticity; myelin; phrenic nerve amplitude; ventilation

INTRODUCTION

Central nervous system (CNS) demyelination is a pathological component of many neurological disorders including multiple sclerosis (MS), the leukodystrophies, (Dutta and Trapp, 2011; Haines et al., 2011; Huang et al., 2011; Eckstein et al., 2012) and spinal cord injuries (Blight, 1983; Guest et al., 2005; Keirstead et al., 2005; Totoiu and Keirstead, 2005; Siegenthaler et al., 2007; Lasiene et al., 2008; Almad et al., 2011; Powers et al., 2012). Primary demyelination usually occurs with damage to the oligodendrocyte whereas secondary demyelination (or Wallerian-like degeneration) follows axonal death (Wisniewski and Bloom, 1975; Franklin and ffrench-Constant, 2008). Primary demyelination can also result in secondary axonal degeneration via immune-mediated transection, loss of trophic support, or a disruption in the balance between energy demand and supply through alterations in ATP production and use (for review see: Dutta and Trapp, 2011). However, despite the cause, demyelination results in slowed or absent saltatory conduction and proteins that are normally distributed tightly around nodes of Ranvier such as contactin-associated proteins (CASPRs) and voltage-gated potassium channels are dispersed across the axolemma (McDonald and Sears, 1970; Felts et al., 1997; Nashmi et al., 2000; Karimi-Abdolrezaee et al., 2006; Ouyang et al., 2010). Following demyelination, attempts at spontaneous axonal remyelination occur and near-normal conduction velocities can be restored in some spared axons as the myelin regenerates (Smith et al., 1979; Blight and Young, 1989; Griffiths and McCulloch, 1983). However, remyelination attempts can fail and functional recovery is often incomplete, especially when oligodendrocytes are exposed to a “hostile” environment and axons are lost (Waxman, 1992; McDonald and Belegu, 2006; Franklin and ffrench-Constant, 2008; Irvine and Blakemore, 2008; Almad et al., 2011; Haines et al., 2011; Huang et al., 2011; Kotter et al., 2011).

Clinical signs associated with demyelination are linked to the lesion site and may include spastic paresis, motor paralysis, ataxia, bladder/bowel dysfunction, fatigue and respiratory impairment. Respiratory impairment associated with spinal demyelination is observed in patients with even mild clinical neurological symptoms (Howard et al., 1992; Redelings et al., 2006; Hirst et al., 2008; Pittock et al., 2011), and is frequently expressed as inspiratory and expiratory muscle weakness (Cooper et al., 1985; Foglio et al., 1994; Buyse et al., 1997; Mutulay et al., 2005; Fry et al., 2007; Karpatkin, 2008). These deficits can be severe, causing significant morbidity and mortality as patients succumb to respiratory (e.g. diaphragm and intercostal) or respiratory-related (e.g. pharyngeal) muscle dysfunction (Redelings et al., 2006; Hirst et al., 2008; Karpatkin, 2008; Zimmer et al., 2008; Terson de Paleville et al., 2011).

Despite the importance of respiratory impairment in demyelinating disease, little is known concerning neural mechanisms underlying this respiratory impairment or how patients compensate for such changes (i.e. compensatory plasticity). Here, we tested the hypothesis that chemically-induced demyelination (ethidium bromide, EB, injected at C₂) of dorsolateral spinal pathways that innervate the diaphragm and forelimbs transiently impairs breathing capacity, the capacity to increase phrenic nerve activity and skilled forelimb function in rats.

Ventilatory capacity was maintained in rats with unilateral demyelination in dorsolateral spinal pathways to respiratory motor neurons. In contrast, the capacity to increase ipsilateral

phrenic motor output (amplitude) was significantly impaired 7 days post-EB. The capacity to increase phrenic activity during chemoreceptor stimulation spontaneously recovers by 14 days post-EB in association with significant spinal cord remyelination.

Skilled forelimb activity was also functionally impaired 7 days post-EB, but exhibited only partial functional recovery 14 days post-injury. Thus, similar to previous investigations, our data suggest that focal spinal demyelination with EB represents a rodent model to study reversible spinal demyelination and its functional consequences (Felts and Smith, 1992; Jeffery and Blakemore, 1997). Further, it provides a useful model for future mechanistic studies concerning the basis of motor (diaphragm and forelimb) impairment, and spontaneous functional recovery via compensatory plasticity (for review see: Mitchell and Johnson, 2003).

EXPERIMENTAL PROCEDURES

Animals

All procedures were approved by the University of Wisconsin's Animal Care and Use Committee. Whole-body plethysmography and neurophysiological recordings were performed in adult Harlan Sprague-Dawley rats (358 ± 9 g) at two time points: 7 ± 2 (Day 7 group) and 14 ± 2 (Day 14 group) days following spinal injection of EB or sham vehicle injections (0.9% NaCl, SHAM). Separate rats were used in each group because the neurophysiological experiments were terminal. Sample sizes for EB treated rats were: 7 days, $n=5$ and 14 days, $n=8$. Sample sizes for SHAM rats were: 7 days, $n=5$ and 14 days, $n=5$. A subset of these rats was used to analyze lesion extent. A separate set of rats was used to study forelimb function pre-injection (EB, $n=6$; SHAM, $n=6$), 7 days post-injection (EB, $n=4$; SHAM, $n=3$), and 14 days post-injection (EB, $n=10$; SHAM, $n=4$).

Ethidium bromide injections

Similar to published protocols (Jeffery and Blakemore, 1997; Blakemore and Franklin, 2008; Mothe and Tator, 2008; Lee et al., 2010b), rats were anesthetized with isoflurane (1-3%) in 100% oxygen delivered via face mask. Dorsal laminectomy at the C₂ cervical spinal segment was performed and a small opening into the dura was made. A 2.0 μ l injection of 0.1% EB or 0.9% NaCl (SHAM) was made unilaterally into the dorsolateral funiculus (right side) 2.0 mm below the C₂ dorsal root entry zone to create a larger lesion than previously reported. The injectate was delivered at 0.8 μ l/min using a Hamilton syringe with a 33 gauge needle. At 7 or 14 days post-injection, rats underwent plethysmography and neurophysiological experiments followed by transcardial perfusion for histological analyses.

Ventilatory measurements

At 7 and 14 days post-injection, ventilatory capacity was assessed in unanesthetized, unrestrained EB and SHAM-injected rats with a whole-body plethysmograph (BUXCO Electronics, Troy, NY). Separate rats were studied at each time point. Whole-body plethysmography allows quantitative measurement of ventilation in unanesthetized, freely-behaving animals while simultaneously controlling inspired gas concentrations. A pressure calibration signal, the plethysmograph temperature, rat body temperature, ambient and chamber pressures, and rat body mass were used to calculate breath-by-breath ventilatory variables using equations described by Drorbaugh and Fenn (1955) as modified by Jacky (1978). Breaths were rejected if there was evidence of pressure fluctuations caused by body movements or sniffing behavior as determined by simultaneous observations of the rats and the plethysmography traces.

Rats were weighed, their body temperatures recorded, and then placed in the plethysmograph (~2 L) while breathing room air (21% oxygen, balance nitrogen) flushed through the chamber at ~3 L/min. Once the rats were quiet but awake after acclimation to the chamber, ventilatory measurements were recorded continuously for 30 min during baseline conditions (21% oxygen, 0% carbon dioxide, balance nitrogen), followed by 15 min of hypoxia (11% oxygen, 0% carbon dioxide, balance nitrogen), and 15 min of hypoxia/hypercapnia (11% oxygen, 7% carbon dioxide, balance nitrogen) to elicit maximal chemoreceptor stimulated breathing. Statistical analyses were performed on data collected during the most quiet 5 min baseline period and the last 5 min of each exposure period. At the conclusion of the study, body temperatures were recorded and the rats underwent neurophysiological experiments (outlined below).

Neurophysiological recordings in anesthetized rats

To assess phrenic motor output in normocapnia, hypoxia, and hypoxia/hypercapnia, SHAM and EB-treated rats (7 or 14 days post-injection) were anesthetized with 2.5-3.5% isoflurane in an induction chamber, maintained with isoflurane delivered via nose cone (50% O₂, balance N₂). A tracheotomy was performed to enable mechanical ventilation (Rodent Respirator, model 683; Harvard Apparatus, Holliston, MA; tidal volume = 2.0-2.5 ml). A femoral vein was cannulated (polyethylene catheter PE50, Intramedic) and the rats were converted to urethane anesthesia over 15-20 min (1.8 g kg⁻¹ i.v., while withdrawing isoflurane). An intravenous infusion was initiated with a 1:2:0.13 mixture of 6% hetastarch in 0.9% sodium chloride, lactated Ringer's solution, and 8.4% sodium bicarbonate (1.5-6.0 ml kg⁻¹ hr⁻¹) to maintain fluid and acid-base balance. Anesthetic depth was tested before and immediately after protocols by lack of any detectable pressor or respiratory neural response to toe pinch.

A flow-through carbon dioxide analyzer was used to measure end-tidal P_{CO₂} (P_{ETCO₂}; Capnogard, Novamatrix, Wallingford, CT, USA). P_{ETCO₂} was maintained at 40-45 mmHg throughout surgery. A bilateral vagotomy was performed (mid-cervical) to prevent entrainment of respiratory neural activity with the ventilator.

To measure blood pressure and arterial blood gases (0.2-0.4 mL/sample; ABL-800 Flex, Radiometer; Westlake, OH), a femoral artery was cannulated (polyethylene catheter PE50, Intramedic) and connected to a pressure transducer (Gould, P231D). Arterial blood gases were taken during baseline, hypoxia (F_IO₂ = 11%; PaO₂ ~35-45 mm Hg) and hypoxia with hypercapnia (F_IO₂ = 11%, PaCO₂ > 90 mm Hg). Rectal temperature was monitored using a thermistor probe thermometer (Fisher Scientific, Pittsburgh, PA, USA) and maintained (37.5 ± 1°C) with a heated surgical table.

Both phrenic nerves were isolated (dorsal approach), cut distally, desheathed and covered with a saline soaked cotton ball until beginning a protocol. After completion of the surgical procedures, a minimum of 1 hour was allowed before experiments commenced.

Neurophysiological Experiments

Rats were paralyzed with pancuronium bromide (2.5 mg kg⁻¹, i.v.). Mineral oil was placed in the cavity and both phrenic nerves were placed on bipolar silver electrodes to record nerve activity (wires spaced 1.1-1.2 mm apart, wire diameter = 0.015 inches). On each side, the same electrode was used in all experiments and the ground was consistently placed on a metal bar located just above the blood pressure transducer. Phrenic neural signals were amplified (10,000X), band-pass filtered (100-10,000 Hz, Model 1800, A-M Systems, Carlsborg, WA, USA), rectified and integrated (Paynter filter, time constant, 50 ms, MA-821, CWE Inc., Ardmore, PA, USA). Integrated phrenic nerve bursts were digitized (8

kHz) and analyzed using WINDAQ data acquisition system (DATAQ Instruments, Akron, OH, USA).

The CO₂ apneic threshold was determined by lowering P_{ETCO₂} (or increasing ventilator rate) until phrenic nerve activity ceased for approximately one minute. The recruitment threshold was determined by slowly increasing the P_{ETCO₂} (or decreasing ventilator rate) until phrenic nerve activity resumed (Bach and Mitchell, 1996). For all experiments, P_{ETCO₂} was held 2 mmHg above the recruitment threshold for approximately 20 min to establish stable neural activity, followed by baseline blood gas samples. Rats were exposed to hypoxia (F_IO₂ = 11%; PaO₂ ~35-45 mm Hg, 5 min), returned to baseline (5 min), exposed to hypoxia with hypercapnia (F_IO₂ = 11%, P_{ETCO₂} = 40 mm Hg above baseline, 5 min), and returned to baseline before ending the protocol. Following experimentation, animals were perfused transcardially with 4% paraformaldehyde.

Assessment of forelimb function

Animals were trained to walk on a 1 meter long horizontal ladder. Pre-injection, 7 and 14 days post-EB injection, rat performance was recorded using a video recorder (Canon FS300). Recordings were later analyzed in slow motion, allowing quantification of the total number of forelimb foot slips while traversing the ladder (5 trials). Only data from the last 20 rungs were analyzed. Any form of miss or foot slip that resulted in the entire paw going below the level of the rung was counted as 1.

Histological analyses

All animals were used for both neurophysiological and plethysmography experiments. Following neurophysiological experiments, rats were transcardially perfused under deep urethane anesthesia with either 2.5% glutaraldehyde or 4% paraformaldehyde in 0.1M phosphate-buffered saline (PBS). Following plethysmography experiments, rats were sacrificed with a lethal dose of Beuthanasia-D Special (Intervet Schering-Plough Animal Health, Summit, NJ) followed by transcardial perfusion with 2.5% glutaraldehyde or 4% paraformaldehyde in 0.1M PBS.

Cervical spinal cords were dissected and the tissue post-fixed in 2.5% glutaraldehyde or 4% paraformaldehyde for 24 hours followed by a post-fix in 1% osmium tetroxide. Tissues were embedded in epon (Electron Microscopy Science, Hatfield, PA), sectioned coronally into 1 μm thick sections, and mounted on slides. Sections were stained with 1% toluidine blue and 1% sodium borate for 3.5 – 4 minutes and washed with distilled water to identify myelin sheaths.

Data analysis

All statistical tests were conducted using SigmaStat 3.5 (SPSS Inc., Chicago, IL, USA) or SigmaPlot 12.0 (Systat Software Inc., San Jose, CA, USA). Differences were considered statistically significant at P<0.05. Data are presented as means ± 1 SEM.

Histological analysis—To quantify the extent of demyelination in vivo, lesions were analyzed using ImageJ 1.45m (NIH). Sections were screened from segment C₂-C₃ for the largest lesion. In this section, EB lesions were outlined and quantified as a percentage of spinal cord white matter at that level. Lesion percentages were compared between SHAM rats and rats at 7 and 14 days post-EB injection with a one-way ANOVA and Fisher's least significant difference (LSD) post hoc test. Linear regression analyses comparing the average ipsi- to contralateral phrenic nerve voltage ratio with lesion extent were performed. Due to unanticipated loss of spinal cord samples during processing, only the averages of 3 and 7 rats were used at 7 and 14 days, respectively.

Awake ventilatory measurements—Ventilatory variables were averaged over 5 min of baseline, hypoxia, and hypoxia/hypercapnia. Measurements included breathing frequency (f), inspiratory time (T_I), tidal volume (V_T), minute ventilation ($\dot{V}_E = V_T \times f$) and the mean inspiratory flow (V_T/T_I). Breathing volumes (V_T , \dot{V}_E , and V_T/T_I) were also normalized per 100 g of body mass.

Body temperatures were compared using a three-way ANOVA with group (EB versus SHAM), experimental time (pre- or post-plethysmography) and time post-injection (7 and 14 days) as factors. Ventilatory parameters were analyzed with a two-way ANOVA between groups (EB versus SHAM rats) at three time points (pre-injection, 7 and 14 days post-injection).

Phrenic nerve responses in anesthetized rats—Apneic and recruitment threshold were compared between groups using t-tests. Integrated phrenic nerve burst amplitudes were averaged over 1 min during baseline, hypoxia and hypoxia/hypercapnia. Phrenic nerve burst amplitude is reported as the voltage of the integrated signal or as the ipsilateral/contralateral ratio. For phrenic amplitudes (voltage), a two-way ANOVA with repeated measures was used with group (SHAM day 7, EB day 7, SHAM day 14, EB day 14) and injection side (contra- or ipsilateral) as factors and voltage as the repeated measure. For ipsilateral/contralateral voltage ratios, a one-way ANOVA was used to compare groups within each condition. Individual comparisons were made using the Fisher's least significant difference (LSD) post hoc test.

Forelimb function—Data from 100 footsteps were recorded from each rat and analyzed using a two-way ANOVA, with rat group (pre-injection, day 7 and 14 EB, and SHAM) and foot (ipsi- and contralateral) as variables, followed by Fisher's least significant difference post-hoc test.

RESULTS

Demyelination lesions

One micron sections from the cervical cord of EB and SHAM-injected rats were stained with toluidine blue at each time point. Images from the injected side of representative rats are shown from each experimental group in Figure 1. The spinal cord contralateral to the injection site had normal myelination in all groups. 7 days post-EB injection, there was a loss of myelin in the dorsolateral funiculus, extending laterally at spinal segments C₂-C₃ (lesion area = $22 \pm 5\%$, Fig. 1A, C). Lesions showed increased extracellular space, with numerous phagocytic cells containing myelin debris 7 days post-injection, similar to that recorded previously (Blakemore, 1982; Graça and Blakemore, 1986; Jeffery and Blakemore, 1997; Penderis et al., 2003; Blakemore and Franklin, 2008). Some axons had thin, degenerating myelin sheaths (Fig. 1B). Lesions were smaller at 14 days as large areas containing axons with thin myelin sheaths, the hallmark of oligodendrocyte remyelination, were seen (lesion area = $12 \pm 2\%$, Fig. 1A-C). The lesion size at 7 and 14 days post-EB differed significantly from each other and from SHAM rats which had no detectable lesions (Day 7 versus 14: $P=0.03$, Day 7 versus SHAM: $P<0.01$, Day 14 versus SHAM: $P=0.02$; Fig. 1). Abundant oligodendrocyte and Schwann cell myelination of intact axons were seen with the characteristics of CNS and PNS myelin at 14 days post-EB (Blakemore, 1982; Graça and Blakemore, 1986; Jeffery and Blakemore, 1997; Penderis et al., 2003; Blakemore and Franklin, 2008; Fig. 1B). Figure 1C shows two additional representative spinal cord tracings from separate rats in all 3 groups (ImageJ), demonstrating the range of the lesions (Day 7: 12-29%; Day 14: 6-18%).

Ventilatory responses

There were no significant differences between rat groups pre-injection in any variable studied (f , T_I , V_T , \dot{V}_E , and V_T/T_I : all $P>0.33$); thus, pre-injection data were combined in subsequent analyses (individual group data not shown). Despite significant unilateral demyelination at C₂, there were no significant differences between groups in baseline f , T_I , V_T , \dot{V}_E , or V_T/T_I at any time point (all $P>0.05$; Fig. 2; T_I and \dot{V}_E not shown). Further, differences in ventilatory responses were not seen during hypoxia or maximal chemoreceptor stimulation at any time point (all $P>0.05$; Fig. 2; T_I and \dot{V}_E not shown). In addition, when V_T , \dot{V}_E , and V_T/T_I were expressed as absolute values (not normalized to body mass), there were no significant differences between groups in any condition at any time point (all $P>0.05$; data not shown). There were no significant differences in pre-versus post-plethysmography body temperatures in either group of rats at any time point (all $P>0.05$; data not shown). These data demonstrate that unilateral demyelination lesions in the dorsolateral C₂ spinal cord have little impact on breathing as the respiratory control system is able to compensate.

Phrenic nerve activity

Apneic and recruitment thresholds were not different between EB and SHAM rats (apneic threshold: SHAM = 38.2 ± 0.8 mm Hg versus EB = 38.9 ± 1.3 mm Hg, $P=0.92$; recruitment threshold: SHAM = 44.8 ± 1.0 mm Hg versus EB = 46.8 ± 0.8 mm Hg, $P=0.38$; note all time points were combined). Further, no significant differences in the amplitude (volts) or the ipsilateral/contralateral amplitude ratios were found in SHAM rats at 7 and 14 days; thus, data were pooled (individual group data not shown, all $P>0.05$; Fig. 3A, B).

Baseline—The ipsilateral nerve amplitudes at 7 and 14 days post-EB were significantly lower than the amplitudes of their corresponding contralateral nerves at both time points (7 days: $P=0.01$, 14 days: $P<0.01$, Fig. 3A) and the ipsilateral phrenic nerve amplitude 7 days post-EB was significantly lower than the ipsilateral amplitude of the SHAM rats and 14 days post-EB (81% and 71%, $P<0.01$ and $P=0.02$, respectively; Fig. 3A). However, the ipsilateral amplitude at 14 days did not differ from the ipsilateral amplitude in SHAM rats ($P=0.06$), indicating at least partial functional improvement from 7 days post-EB during baseline breathing. The contralateral phrenic nerve amplitude 7 days post-EB was significantly lower than the contralateral amplitude 14 days post-EB (41%, $P=0.03$; Fig. 3A), but did not differ from contralateral amplitude of SHAM rats ($P=0.11$; Fig. 3A); contralateral amplitude was not different than SHAM levels at day 14 ($P>0.05$, Fig. 3A).

Hypoxia and hypoxia/hypercapnia—With chemosensory stimulation, ipsilateral phrenic nerve amplitude 7 days post-EB was significantly lower versus ipsilateral amplitude in SHAM rats (hypoxia: 76%, $P<0.001$; hypoxia/hypercapnia: 72%, $P<0.001$) and ipsilateral amplitude 14 days post-EB (hypoxia: 71%, $P<0.01$; hypoxia/hypercapnia: 67%, $P<0.01$; Fig. 3A). Further, the ipsilateral phrenic amplitude 7 days post-EB was significantly lower than the contralateral amplitude at the same time point (hypoxia: 71%, hypoxia/hypercapnia 68%; both $P<0.001$; Fig. 3A). Contralateral phrenic nerve amplitude 7 days post-EB did not differ significantly from contralateral amplitude of any other rat groups (both $P>0.05$) and within the SHAM and 14 days post-EB groups, the ipsi- and contralateral amplitudes did not differ (both $P>0.05$).

Ipsi- to contralateral ratios of phrenic activity—When expressed as a ratio of ipsilateral to contralateral phrenic burst amplitudes in a given rat, EB was noted to decrease ipsilateral output transiently. A ratio of ipsilateral to contralateral voltage in a rat without impairment on either side is expected to be 1.0 since both sides should have similar outputs. However, as the ipsilateral phrenic nerve becomes increasingly affected, and the

contralateral phrenic nerve remains unaffected, the ratio should dip below 1.0. Average amplitude ratios in SHAM rats were 0.95 ± 0.04 , 0.95 ± 0.05 , and 0.95 ± 0.06 in baseline, hypoxia and hypoxia/hypercapnia, respectively; none of these values were significantly different from 1.0 or from one another (all $P > 0.05$; Fig. 3B). Average ipsi/contralateral ratios at day 7 post-EB were significantly lower than SHAM rats (69%; $P < 0.001$) and 14 days post-injection during baseline conditions (56%; $P = 0.02$; Fig. 3B). However, the baseline ratios at day 14 did not return to SHAM levels ($P = 0.03$; Fig. 3B), indicating only a partial recovery at resting conditions. Ipsi/contralateral ratios were significantly lower at 7 days when compared to SHAM rats and rats 14 days post-EB in hypoxia (71% and 67%, respectively; $P < 0.001$, and $P < 0.01$, respectively) and hypoxia/hypercapnia (64% and 61%, respectively; $P < 0.01$ and $P = 0.02$, respectively; Fig. 3B). Thus, EB elicits considerable impairment in phrenic nerve output ipsilateral to injury, and this impairment recovers during chemosensory activation by 14 days post-EB.

Multivariate analyses of breathing conditions (baseline, hypoxia, and hypoxia/hypercapnia), time post-EB, percent white matter involvement and ipsilateral to contralateral phrenic nerve amplitude ratios at 7 and 14 days, respectively, revealed highly significant correlations ($P < 0.001$, $r^2 = 0.84$; data not shown). When conditions were assessed individually, average baseline phrenic nerve ratios were significantly correlated to lesion extent ($r^2 = 0.99$, $P = 0.02$; Fig. 4). Although these trends continued in hypoxia and hypoxia/hypercapnia (both $r^2 = 0.98$), regressions were no longer statistically significant (both $P = 0.10$; Fig. 4).

Horizontal ladder walking

The average number of forelimb foot slips during 100 steps on a horizontal ladder is shown in Figure 5. There were no significant differences in forelimb slips in either limb between SHAM and EB groups pre-injection, thus, these groups were subsequently combined (all $P > 0.05$; data not shown). There were no significant differences between ipsi- and contralateral forelimbs at any time in SHAM animals (day 7: $P = 0.92$, day 14: $P = 0.85$), nor were there differences in SHAM rats over time when compared to pre-injection values (all $P > 0.50$; Fig. 5). Contralateral limb function of EB-injected rats was similar to SHAM rats (7 days: $P = 0.24$, 14 days: $P = 0.49$; Fig. 5). At 7 and 14 days post-injection, the ipsilateral limb in EB rats had significantly more foot slips than pre-injection values (both $P < 0.001$), and more than the contralateral limb in EB-injected rats at each time point (both $P < 0.001$; Fig. 5). Although the ipsilateral limb of EB-injected rats had less slips at 14 days versus the ipsilateral limb at 7 days ($P < 0.001$; Fig. 5), the number of foot slips remained significantly higher than pre-injection or SHAM levels (both $P < 0.001$, Fig. 5), indicating continued forelimb impairment.

DISCUSSION

Although ventilatory capacity is maintained in rats with unilateral demyelination of dorsolateral spinal pathways, phrenic inspiratory motor output (amplitude) was reduced substantially on the side of injury. This functional deficit was transient, as phrenic amplitude ratios returned to normal during chemosensory activation by 14 days post-injury. Why impaired phrenic nerve output was not reflected in diminished breathing capacity at 7 days post-EB is unclear, but suggests an impressive degree of functional compensation (Mitchell and Johnson, 2003). Demyelination of these same pathways also impaired forelimb motor function which significantly improved by 14 days post-EB injection but did not reach SHAM levels. The continued forelimb impairment may reflect dominant demyelination in the dorsolateral spinal cord (Fig. 1), where greater effects on forelimb function are expected (versus ventrolateral for phrenic innervation; Feldman et al., 1985; Webb and Muir, 2005), the relative complexity of the forelimb task (involving many muscles), the continued loss of axons (through Wallerian-like degeneration) contributing to such a complex, coordinated

activity, or a fundamental difference in the sensitivity of these motor tasks to spinal myelination. Regardless, we demonstrate deficiencies in respiratory (phrenic) and forelimb motor activity associated with demyelination in dorsolateral spinal pathways, thus establishing a model to study mechanisms of respiratory motor impairment associated with spinal demyelination, mechanisms of spontaneous functional recovery, and the efficacy of new therapeutic interventions intended to reduce the severity or duration of relapsing clinical disease.

Ethidium bromide demyelination

Gliotoxin-induced demyelination of the dorsal funiculus with EB has been studied extensively (Blakemore, 1982; Graça and Blakemore, 1986; Jeffery and Blakemore, 1997; Blakemore and Franklin, 2008; Mothe and Tator, 2008; Lee et al., 2010b). Although our lesions did not encompass all respiratory tracts, this investigation is the first report of injections targeting dorsolateral cervical spinal tracts to respiratory motor nuclei (for review see: Lee and Fuller, 2011).

In the EB demyelination model (for review see: Blakemore and Franklin, 2008), oligodendrocytes show signs of toxicity within 24 hours, resulting in extensive demyelination 7-14 days post-injection (Blakemore, 1982; Jeffery and Blakemore, 1997). However, remyelination occurs spontaneously; Schwann cells are present within 7 days and extensive remyelination is observed by 13 days (Blakemore, 1982; Graça and Blakemore, 1986; Sallis et al., 2006; Bondan et al., 2010). Our results are consistent with these earlier reports as spinal tracts were demyelinated at 7 days post-EB, with remyelination observed at 14 days. Both extensive Schwann cell and oligodendrocyte remyelination of intact axons were observed, consistent with previous reports (Blakemore and Franklin, 2008; Bondan et al., 2010). Although axonal degeneration is associated with toxin-induced demyelination (for review see: Blakemore and Franklin, 2008), the substantial (yet not complete) remyelination in our rats by day 14 post-EB is more likely consistent with remyelination of intact, yet previously demyelinated spinal axons. Here, we did not study the extent of axonal regeneration versus remyelination in sufficient detail to determine the precise contribution of each to phrenic amplitude recovery. Although multiple factors could contribute to recovery of phrenic nerve activity, the general consensus is that spinal remyelination is the most likely mechanism to account for physiological improvement. However, we cannot rule out the possibility that some axon retraction and/or degeneration occurred subsequent to the EB injection, and that regrowth contributed to functional recovery. The inverse correlation between phrenic activity and lesion area does not discriminate between these possibilities. Regardless, one fundamental conclusion is robust - profound impairment of phrenic motor output does not necessarily compromise ventilatory capacity. Further, phrenic motor deficits recover in parallel with substantial, but partial remyelination of lesioned spinal tracts. Nevertheless, despite deficits in phrenic motor output, the respiratory system demonstrates a remarkable degree of compensation, most likely due to increased contributions from accessory respiratory muscles (e.g. intercostal muscles), particularly during respiratory challenge (Bolser et al., 2009; Golder et al., 2011).

We had intended to create a more ventral lesion based on the depth of injections. However, dorsolateral lesions were consistent in all rats, possibly because injectate travelled up the needle tract following a path of least resistance or compression of the spinal cord as the needle was inserted. Regardless, visualization of our lesions confirmed that they were similar among rats.

Respiratory motor impairment

Ventilation in rats is a complex physiologic process involving respiratory rhythm generation, chemo- and mechanosensory reflexes, and activation of many respiratory muscles. Dorsolateral lesions would at least partially demyelinate spinal tracts innervating phrenic motor neurons, although there is reason to believe that only the most rostral phrenic motor neurons were affected (Feldman et al., 1985; Ling et al., 1994; Fuller et al., 2009). Regardless of these lesions, no impairment of breathing was observed during baseline or chemoreceptor stimulated breathing. Although spinal projections to phrenic motor neurons are found throughout the white matter, most pathways innervating ipsilateral phrenic motor neurons are located in the lateral funiculus whereas pathways crossing the spinal cord to contralateral motor neurons are mainly found in the ventral funiculus (Feldman et al., 1985; Lipski et al., 1994; Fuller et al., 2009; Lee and Fuller, 2011). Our lesions did not encompass all of these pathways, yet they were sufficient to impair ipsilateral phrenic motor output. Why this impairment was not reflected in breathing capacity is unknown, but suggests a substantial degree of compensatory plasticity, shifting the balance from the diaphragm to other respiratory muscles as discussed above. Indeed, numerous prior studies have investigated plasticity and adaptive responses following loss of diaphragm function from injury (for review see: Sharma et al., 2011). Although we have not explored these possibilities at this time, our previous studies suggest complete CNS dysmyelination is associated with ventilatory impairment and phrenic nerve output abnormalities (Long Evans shaker [les] rat; Johnson et al., 2010). Thus, the effect of demyelination on ventilatory function may be associated with lesion extent.

Motor evoked potentials in the dorsal funiculus are reduced with demyelination (Lee et al., 2010b). Conduction is slowed, at least in part, by exposed potassium channels at the juxtaparanodal regions. Potassium efflux through these channels is sufficient to cause conduction block by preventing depolarization and action potential generation at the node of Ranvier (Chiu and Ritchie, 1980; Sherratt et al., 1980; Waxman, 1992; Nashmi et al., 2000; Ouyang et al., 2010; Sun et al., 2010; Lueng et al., 2011). We did not investigate axonal conduction per se. However, phrenic burst amplitude, an index of the summated action potentials from phrenic motor neurons, was greatly diminished ipsilateral to the lesion, presumably through reduced conduction secondary to demyelination of dorsolateral pathways to phrenic motor neurons.

One limitation of the methods used here is the difficulty in comparing integrated phrenic activity among rat groups (expressed as a voltage). Thus, we represented data both as an absolute value (voltage) and as a ratio of the ipsi- and contralateral sides to injection. In SHAM rats, the ipsi/contralateral ratio was very near 1.0 ($0.95 \pm 0.04-0.06$), indicating that the recording methods were comparable on both sides. Further, compiled data from multiple different studies in our laboratory group confirm that the absolute voltage within a singular rat strain is similar across studies when measured in similar conditions (unpublished data). An important caveat is that the individual performing the neurophysiological experiments must be experienced with the methods employed here.

In support of this approach, comparisons of ipsi- versus contralateral nerve activity are widely used in the spinal cord injury literature (Kajana and Goshgarian, 2009; Fuller et al., 2009; Lee et al., 2010a). Regardless, we chose to present data both as an absolute voltage of the integrated phrenic neurogram and as a ratio of ipsi- to contralateral integrated activity. Conclusions drawn from both analyses are essentially the same.

Although contralateral baseline nerve amplitude at 7 days post-injection was not significantly different from the contralateral nerve amplitude of SHAM rats, it was significantly reduced from the contralateral amplitude at 14 days post-injection. However,

contralateral amplitude at 7 days post-injection quickly returned to normal levels with chemosensory activation (<5 min), demonstrating that these pathways were substantially intact. On the other hand, whereas it is unlikely that we demyelinated crossed-spinal pathways (Lipski et al., 1994), some contralateral axons may have been affected post-EB injections.

Forelimb (somatic) motor impairment

EB-induced lesions in the dorsal funiculus of rats impair locomotor activity (Zhang et al., 2012). Here, we confirm compromised locomotor activity associated with EB-induced dorsolateral spinal demyelination as demonstrated by impaired performance in the horizontal ladder walking test. Although forelimb deficits improved from 7 to 14 days, they did not return to normal levels, indicating at least a partial recovery by 14 days. This time frame is more consistent with remyelination of intact axons versus axonal regrowth over long distances. We did not determine the precise roles of either process in forelimb recovery.

Spinal contusion injuries in rats are associated with spinal demyelination and hind limb motor deficits which improve, but do not return to normal by ~ 12 weeks post-injury (James et al., 2011). Strategies to enhance remyelination in acute spinal injuries improve functional recovery, but these treatments are not effective in chronic injuries (Keirstead et al, 2005; Karimi-Abdolrezaee et al., 2006; Cao et al., 2010). Although the contusion model differs significantly from EB-induced demyelination, both models may share similar pathological mechanisms that prevent full motor recovery including demyelination and axonal degeneration. Since our dorsolateral lesion affects many sensory spinal tracts as well as motor pathways to respiratory and somatic muscles, sensory dysfunction may persist at 14 days post-EB, resulting in longer forelimb impairment. This hypothesis remains to be tested.

CONCLUSIONS

Although the mechanistic basis of impaired respiratory and somatic motor function following dorsal spinal demyelination is not yet known, novel insights were gained: 1) phrenic motor output is impaired without impairment of overall breathing capacity, once again suggesting a remarkable degree of compensatory plasticity in this critical homeostatic motor control system, and 2) respiratory and forelimb motor function differ appreciably in their sensitivity to dorsolateral spinal demyelination since the former, but not the latter, rapidly recovers. Although this study does not directly demonstrate a causal relationship between return of phrenic motor function and spinal remyelination, the strong correlation is highly suggestive of such a relationship. We conclude that EB-induced demyelination is a useful model to study transient respiratory motor impairment, mechanisms underlying respiratory compensatory plasticity, and the possibility of new therapeutic interventions that reduce the severity and/or duration of impaired function associated with remitting/relapsing neurological diseases.

Acknowledgments

The project described was supported by the Clinical and Translational Science Award (CTSA) program, previously through the National Center for Research Resources (NCRR) grant 1UL1RR025011, and now by the National Center for Advancing Translational Sciences (NCATS), grant 9U54TR000021 (RA Johnson). The content is solely the responsibility of the authors and does not necessarily represent the official views of the NIH. GS Mitchell was supported by NIH HL69064. NL Nichols was supported by the NHLBI Respiratory Neurobiology Training Grant T32 HL007654 and the Francis Families Foundation.

ABBREVIATIONS

EB	ethidium bromide
f	breathing frequency
T_I	inspiratory time
V_T	tidal volume
V_E	minute ventilation (the product of breathing frequency and tidal volume)
V_T/T_I	mean inspiratory flow
P_{ETCO₂}	partial pressure of end-tidal carbon dioxide
F_IO₂	inspiratory fraction of oxygen
PaO₂	arterial partial pressure of oxygen

REFERENCES

- Almad A, Sahinkaya FR, McTigue DM. Oligodendrocyte fate after spinal cord injury. *Neurotherapeutics*. 2011; 8(2):262–273. [PubMed: 21404073]
- Bach KB, Mitchell GS. Hypoxia-induced long-term facilitation of respiratory activity is serotonin dependent. *Respir Physiol*. 1996; 104(2-3):251–260. [PubMed: 8893371]
- Blakemore WF. Ethidium bromide induced demyelination in the spinal cord of the cat. *Neuropathol Appl Neurobiol*. 1982; 8(5):365–375. 1982. [PubMed: 7177337]
- Blakemore WF, Franklin RJ. Remyelination in experimental models of toxin-induced demyelination. *Curr Top Microbiol Immunol*. 2008; 318:193–212. [PubMed: 18219819]
- Blight AR. Cellular morphology of chronic spinal cord injury in the cat: analysis of myelinated axons by line-sparing. *Neuroscience*. 1983; 10(2):521–543. [PubMed: 6633870]
- Blight AR, Young W. Central axons in injured cat spinal cord recover electrophysiological function following remyelination by Schwann cells. *J Neurol Sci*. 1989; 91:15–34. [PubMed: 2746287]
- Bolser DC, Jefferson SC, Rose MJ, Tester NJ, Reier PJ, Fuller DD, Davenport PW, Howland DR. Recovery of airway protective behaviors after spinal cord injury. *Respir Physiol Neurobiol*. 2009; 169(2):150–156. [PubMed: 19635591]
- Bondan EF, Lallo MA, Martins MFM, Graça DL. Schwann cell expression of an oligodendrocyte-like remyelinating pattern after ethidium bromide injection in the rat spinal cord. *Arq Neuropsiquiatr*. 2010; 68(5):783–787. [PubMed: 21049194]
- Buyse B, Demedts M, Meekers J, Vandegaer L, Rochette M, Kerkhofs L. Respiratory dysfunction in multiple sclerosis: a prospective analysis of 60 patients. *Eur Respir J*. 1997; 10(1):139–145. [PubMed: 9032506]
- Cao Q, He Q, Wang Y, Cheng X, Howard RM, Zhang Y, DeVries WH, Shields CB, Magnuson DS, Xu XM, Kim DH. Transplantation of ciliary neurotrophic-factor expressing adult oligodendrocyte precursor cells promotes remyelination and functional recovery after spinal cord injury. *J Neurosci*. 2010; 30:2989–3001. [PubMed: 20181596]
- Chiu SY, Ritchie JM. Potassium channels in nodal and internodal axonal membrane of mammalian myelinated fibres. *Nature*. 1980; 284:170–171. [PubMed: 6244497]
- Cooper CB, Trend PS, Wiles CM. Severe diaphragm weakness in multiple sclerosis. *Thorax*. 1985; 40(8):633–634. [PubMed: 4035638]
- Drorbaugh JE, Fenn WO. A barometric method for measuring ventilation in newborn infants. *Pediatrics*. 1955; 16:81–87. [PubMed: 14394741]
- Dutta R, Trapp BD. Mechanisms of neuronal dysfunction and degeneration in multiple sclerosis. *Prog Neurobiol*. 2011; 93:1–12. [PubMed: 20946934]
- Eckstein C, Saidha S, Levy M. A differential diagnosis of central nervous system demyelination: beyond multiple sclerosis. *J Neurol*. 2012; 259(5):801–816. [PubMed: 21932127]

- Feldman JL, Loewy AD, Speck DF. Projections from the ventral respiratory group to phrenic and intercostal motoneurons in cat: an autoradiographic study. *J Neurosci.* 1985; 5:1993–2000. [PubMed: 3926961]
- Felts PA, Baker T, Smith KJ. Conduction in segmentally demyelinated mammalian central axons. *J Neurosci.* 1997; 17:7267–7277. [PubMed: 9295373]
- Felts PA, Smith KJ. Conduction properties of central nerve fibers remyelinated by Schwann cells. *Brain Res.* 1992; 574:178–192. [PubMed: 1638392]
- Foglio K, Clini E, Facchetti D, Vitacca M, Maragoni S, Bonomelli S, Ambrosino N. Respiratory muscle function and exercise capacity in multiple sclerosis. *Eur Respir J.* 1994; 7(1):23–28. [PubMed: 8143827]
- Franklin RJM, French-Constant C. Remyelination in the CNS: from biology to therapy. *Nat Rev Neurosci.* 2008; 9(11):839–855. [PubMed: 18931697]
- Fry DK, Pfalzer LA, Chokshi AR, Wagner MT, Jackson ES. Randomized control trial of effects of a 10-week inspiratory muscle training program on measures of pulmonary function in persons with multiple sclerosis. *J Neurol Phys Ther.* 2007; 31(4):162–172. [PubMed: 18172412]
- Fuller DD, Sandhu MS, Doperalski NJ, Lane MA, White TE, Bishop MD, Reier PJ. Graded unilateral cervical spinal cord injury and respiratory motor recovery. *Respir Physiol Neurobiol.* 2009; 165:245–253. [PubMed: 19150658]
- Golder FJ, Fuller DD, Lovett-Barr MR, Vinit S, Resnick DK, Mitchell GS. Breathing patterns after mid-cervical spinal contusion in rats. *Exp Neurol.* 2011; 231(1):97–103. [PubMed: 21683697]
- Graça DL, Blakemore WF. Delayed remyelination in rat spinal cord following ethidium bromide injection. *Neuropathol Appl Neurobiol.* 1986; 12:593–605. [PubMed: 3561693]
- Griffiths IR, McCulloch MC. Nerve fibres in spinal cord impact injuries. Part I. Changes in the myelin sheath during the initial 5 weeks. *J Neurol Sci.* 1983; 58:335–349. [PubMed: 6842262]
- Guest JD, Heister ED, Bunge RP. Demyelination and Schwann cell responses adjacent to injury epicenter cavities following chronic human spinal cord injury. *Exp Neurol.* 2005; 192(2):384–393. [PubMed: 15755556]
- Haines JD, Inglese M, Casaccia P. Axonal damage in multiple sclerosis. *Mt. Sinai J Med.* 2011; 78(2): 231–243. [PubMed: 21425267]
- Hirst C, Swingler R, Compston DA, Ben-Schlomo Y, Robertson NP. Survival and cause of death in multiple sclerosis: a prospective population-based study. *J Neurol Neurosurg Psychiatry.* 2008; 79(9):1016–1021. [PubMed: 18303108]
- Howard RS, Wiles CM, Hirsch NP, Loh L, Spencer GT, Newsome-Davis J. Respiratory involvement in multiple sclerosis. *Brain.* 1992; 115(Pt2):479–494. [PubMed: 1606478]
- Huang JK, Fancy SP, Zhao C, Rowitch DH, French-Constant C, Franklin RJ. Myelin regeneration in multiple sclerosis: targeting endogenous stem cells. *Neurotherapeutics.* 2011; 8(4):650–658. [PubMed: 21904791]
- Irvine KA, Blakemore WF. Remyelination protects axons from demyelination-associated axon degeneration. *Brain.* 2008; 131:1464–1477. [PubMed: 18490361]
- Jacky JP. A plethysmograph for long-term measurements of ventilation in unrestrained animals. *J Appl Physiol.* 1978; 45:644–647. [PubMed: 101497]
- James ND, Bartus K, Grist J, Bennett DLH, McMahon SB, Bradbury EJ. Conduction failure following spinal cord injury: functional and anatomical changes from acute to chronic stages. *J Neurosci.* 2011; 31(50):18543–18555. [PubMed: 22171053]
- Jeffery ND, Blakemore WF. Locomotor deficits induced by experimental spinal cord demyelination are abolished by spontaneous remyelination. *Brain.* 1997; 120:27–37. [PubMed: 9055795]
- Johnson RA, Baker-Herman TL, Duncan ID, Mitchell GS. Ventilatory impairment in the dysmyelinated Long Evans shaker (les) rat. *Neuroscience.* 2010; 169(3):1105–1114. [PubMed: 20542092]
- Kajana S, Goshgarian HG. Administration of phosphodiesterase inhibitors and an adenosine A1 receptor antagonist induces phrenic nerve recovery in high cervical spinal cord injured rats. *Exp Neurol.* 2009; 210(2):671–680. [PubMed: 18289533]

- Karimi-Abdolrezaee S, Eftekharpour E, Wang J, Morshead CM, Fehlings MG. Delayed transplantation of adult neural precursor cells promotes remyelination and functional neurological recovery after spinal cord injury. *J Neurosci*. 2006; 26:3377–3389. [PubMed: 16571744]
- Karpatkin H. Respiratory changes in multiple sclerosis. *J Neurol Phys Ther*. 2008; 32(2):105. [PubMed: 18645300]
- Keirstead HS, Nistor G, Bernal G, Totoiu M, Cloutier F, Sharp K, Steward O. Human embryonic stem cell-derived oligodendrocyte progenitor cell transplants remyelinate and restore locomotion after spinal cord injury. *J Neurosci*. 2005; 25:4694–4705. [PubMed: 15888645]
- Kotter MR, Stadelmann C, Hartung HP. Enhancing remyelination in disease – can we wrap it up? *Brain*. 2011; 134(7):1882–1900. [PubMed: 21507994]
- Lasiene J, Shupe L, Perlmutter S, Horner P. No evidence for chronic demyelination in spared axons after spinal cord injury in a mouse. *J Neurosci*. 2008; 28(15):3887–3896. [PubMed: 18400887]
- Lee KZ, Sandhu MS, Dougherty BJ, Reier PJ, Fuller DD. Influence of vagal afferents on supraspinal and spinal respiratory activity following cervical spinal cord injury in rats. *J Appl Physiol*. 2010a; 109(2):377–387. [PubMed: 20507963]
- Lee KH, Yoon DH, Chung M-A, Sohn J-H, Lee H-J, Lee BH. Neuroprotective effects of mexiletine on motor evoked potentials in demyelinated rat spinal cords. *Neurosci Res*. 2010b; 67:59–64. [PubMed: 20096736]
- Lee KZ, Fuller DD. Neural control of phrenic motoneuron discharge. *Respir Physiol Neurobiol*. 2011; 179(1):71–79. [PubMed: 21376841]
- Ling L, Bach KB, Mitchell GS. Serotonin reveals ineffective spinal pathways to contralateral phrenic motoneurons in spinally hemisectioned rats. *Exp Brain Res*. 1994; 101(1):35–43. [PubMed: 7843300]
- Lipski J, Zhang X, Kruszewska B, Kanjhan R. Morphological study of long axonal projections of ventral medullary inspiratory neurons in the rat. *Brain Res*. 1994; 640:171–184. [PubMed: 8004446]
- Lueng G, Sun W, Brookes S, Smith D, Shi R. Potassium channel blocker, 4-aminopyridine-3-methanol, restores axonal conduction in spinal cord of an animal model of multiple sclerosis. *Exp Neurol*. 2011; 227:232–235. [PubMed: 21093437]
- McDonald WI, Sears TA. The effects of experimental demyelination on conduction in the central nervous system. *Brain*. 1970; 93:583–598. [PubMed: 4319185]
- McDonald JW, Belegu V. Demyelination and remyelination after spinal cord injury. *J Neurotrauma*. 2006; 23(304):345–359. [PubMed: 16629621]
- Mitchell GS, Johnson SM. Neuroplasticity in respiratory motor control. *J Appl Physiol*. 2003; 94(1): 358–374. [PubMed: 12486024]
- Mothe AJ, Tator CH. Transplanted neural stem/progenitor cells generate myelinating oligodendrocytes and Schwann cells in spinal cord demyelination and dysmyelination. *Exp Neurol*. 2008; 213:176–190. [PubMed: 18586031]
- Mutulay FK, Gürses HN, Saip S. Effects of multiple sclerosis on respiratory functions. *Clin Rehabil*. 2005; 19(4):426–432. [PubMed: 15929512]
- Nashmi R, Jones OT, Fehlings MG. Abnormal axonal physiology is associated with altered expression and distribution of Kv1.1 and Kv1.2 K⁺ channels after chronic spinal cord injury. *Eur J Neurosci*. 2000; 12:491–506. [PubMed: 10712629]
- Ouyang H, Sun W, Fu Y, Li J, Cheng JX, Nauman E, Shi R. Compression induces acute demyelination and potassium channel exposure in spinal cord. *J Neurotrauma*. 2010; 27(6):1109–1120. [PubMed: 20373847]
- Penderis J, Shields SA, Franklin RJM. Impaired remyelination and depletion of oligodendrocyte progenitors does not occur following repeated episodes of focal demyelination in the rat central nervous system. *Brain*. 2003; 126:1382–1391. [PubMed: 12764059]
- Pittock SJ, Weinschenker BG, Wijdicks EFM. Mechanical ventilation and tracheostomy in multiple sclerosis. *J Neurol Neurosurg Psychiatry*. 2011; 75:1331–1333. [PubMed: 15314126]
- Powers BE, Lasiene J, Plemel JR, Shupe L, Perlmutter SI, Telzlaff W, Horner PJ. Axonal thinning and extensive remyelination without chronic demyelination in spinal injured rats. *J Neurosci*. 2012; 32(15):5120–5125. [PubMed: 22496557]

- Redelings MD, McCoy L, Sorvillo F. Multiple sclerosis mortality and patterns of comorbidity in the United States from 1990-2001. *Neuroepidemiology*. 2006; 26(2):102–107. [PubMed: 16374035]
- Sallis ES, Mazzanti CM, Mazzanti A, Periera LA, Arroteia KF, Fustigatto R, Pelizzari C, Rodrigues A, Graça DL. OSP-Immunofluorescent remyelinating oligodendrocytes in the brainstem of toxically-demyelinated Wistar rats. *Arg Neuropsiquiatr*. 2006; 64(2A):240–244.
- Sharma H, Alilain WJ, Sadhu A, Silver J. Treatments to restore respiratory function after spinal cord injury and their implications for regeneration, plasticity and adaptation. *Exp Neurol*. 2011; 235:18–25. [PubMed: 22200541]
- Sherratt RM, Bostock H, Sears TA. Effects of 4-aminopyridine on normal and demyelinated mammalian nerve fibres. *Nature*. 1980; 283:570–572. [PubMed: 7354839]
- Siegenthaler MM, Tu MK, Keirstead HS. The extent of myelin pathology differs following contusion and transection spinal cord injury. *J Neurotrauma*. 2007; 24(10):1631–1646. [PubMed: 17970626]
- Smith KJ, Blakemore WF, McDonald WI. Central remyelination restores secure conduction. *Nature*. 1979; 280:395–396. [PubMed: 460414]
- Sun W, Smith D, Fu Y, Chang JX, Bryn S, Borgens R, Shi R. Novel potassium channel blocker, 4-AP-3-MeOH, inhibits fast potassium channels and restores axonal conduction in injured guinea pig spinal cord white matter. *J Neurophysiol*. 2010; 103:469–478. [PubMed: 19923250]
- Terson de Paleville DGL, McKay WB, Folz RJ, Ovechkin AV. Respiratory motor control disrupted by spinal cord injury: mechanisms, evaluation, and restoration. *Transl Stroke Res*. 2011; 2(4):463–473. [PubMed: 22408690]
- Totoiu MO, Keirstead HS. Spinal cord injury is accompanied by chronic progressive demyelination. *J Comp Neurol*. 2005; 486(4):373–383. [PubMed: 15846782]
- Waxman SG. Demyelination in spinal cord injury and multiple sclerosis: what can we do to enhance functional recovery? *J Neurotrauma*. 1992; 9:S105–117. [PubMed: 1588601]
- Webb AA, Muir GD. Sensorimotor behavior following incomplete cervical spinal cord injury in the rat. *Behav Brain Res*. 2005; 165:147–159. [PubMed: 16157393]
- Wisniewski HM, Bloom BR. Primary demyelination as a nonspecific consequence of a cell-mediated immune reaction. *J Exp Med*. 1975; 141:346–359. [PubMed: 803545]
- Zhang Y-J, Zhang W, Lin C-G, Ding Y, Huang S-F, Wu J-L, Li Y, Dong H, Zeng Y-S. Neurotrophin-3 gene modified mesenchymal stem cells promote remyelination and functional recovery in the demyelinated spinal cord of rats. *J Neurol Sci*. 2012; 313:64–74. [PubMed: 21996274]
- Zimmer MB, Nantwi K, Goshgarian HG. Effect of spinal cord injury on the neural regulation of respiratory function. *Exp Neurol*. 2008; 209:399–406. [PubMed: 17603041]

- Spinal ethidium bromide injections produced transient dorso-lateral demyelination.
- Ventilation did not change with ethidium bromide (EB) demyelination.
- Ipsilateral phrenic nerve amplitude was transiently reduced post-EB.
- Ipsilateral limb function was continually impaired post-EB.
- EB provides a reversible demyelination model to study compensatory motor plasticity.

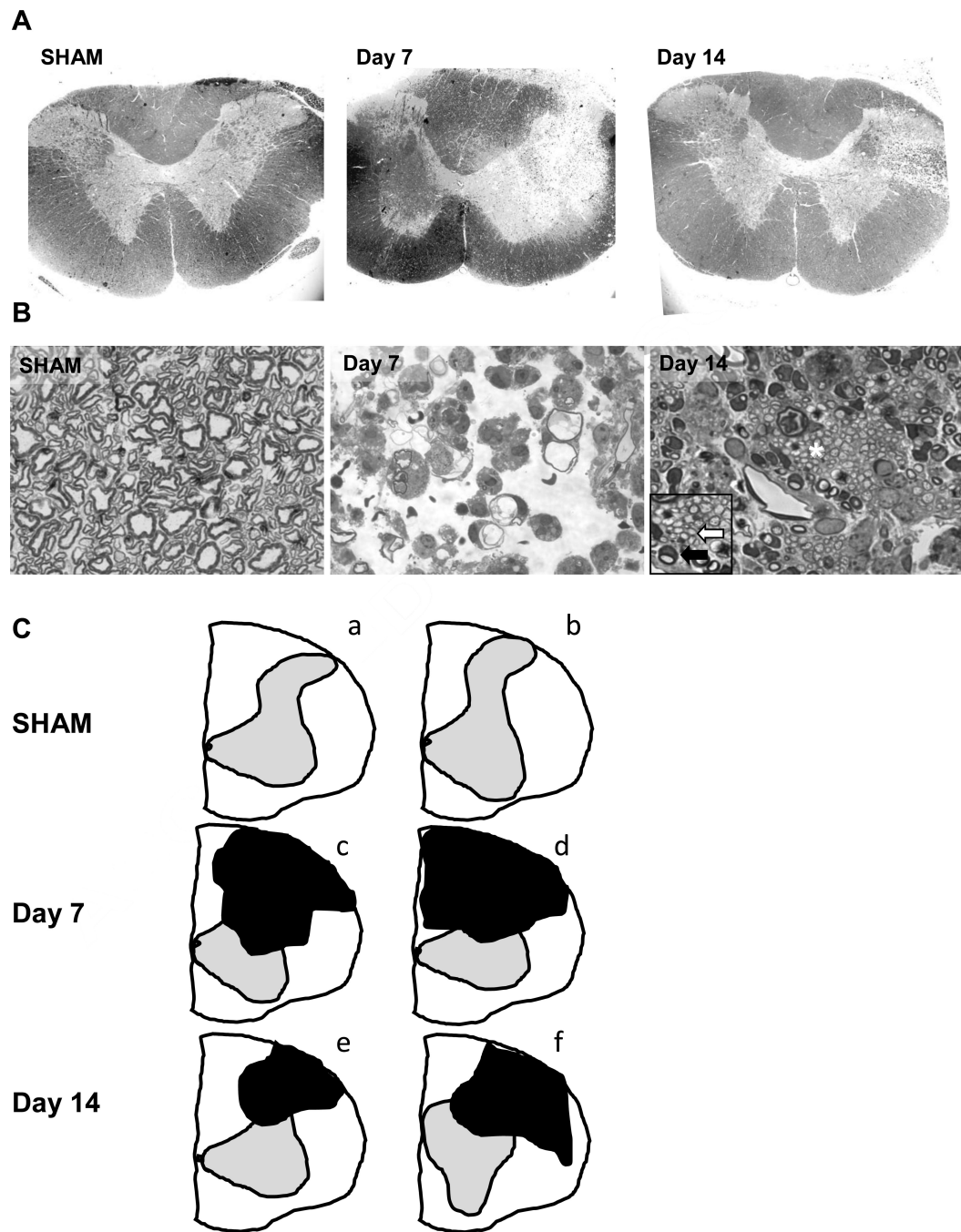


Figure 1.

(A) Toluidine blue staining of cervical spinal segments (C₂-C₃) from a representative SHAM-injected rat, 7, and 14 days post-EB injection. Images are taken at the segment where the largest cross-sectional area of the lesion was visualized. (B) Ipsilateral spinal cord images of representative rats taken within the white matter lesions. No demyelination was seen in the contralateral spinal cord sections of EB-injected rats or on either side of SHAM-injected rats at any time point. At 7 days post-EB injection, there was significant demyelination of the dorsolateral tracts ($21.7 \pm 5.1\%$ of the white matter, $P < 0.01$ versus SHAM; one-way ANOVA, A, C), with many phagocytic cells and myelin debris (B). By 14

days, the lesion was significantly smaller and extensive remyelination of existing axons was seen. The inset (enlarged area marked with asterisk) shows numerous thinly remyelinated axons typical of oligodendrocyte repair (white arrow), while Schwann cells generating PNS myelin are seen at the periphery (dark arrow) (lesion area = $12.0 \pm 1.5\%$, $P=0.016$ versus day 7 group, $P=0.03$ versus SHAM; one-way ANOVA, A-C). (C) Two additional representative images of cervical segments reproduced in ImageJ and demonstrating the range of lesions which are depicted as black objects (SHAM (a-b): no obvious lesions; Day 7 (c-d): 12-29%; Day 14 (e-f): 6-18% of the white matter). Sections depicted had the largest cross-sectional area occupied by the lesion. Figures 1A and 1C: 4X, 1B: 100X, Inset: 200X magnification.

\$watermark-text

\$watermark-text

\$watermark-text

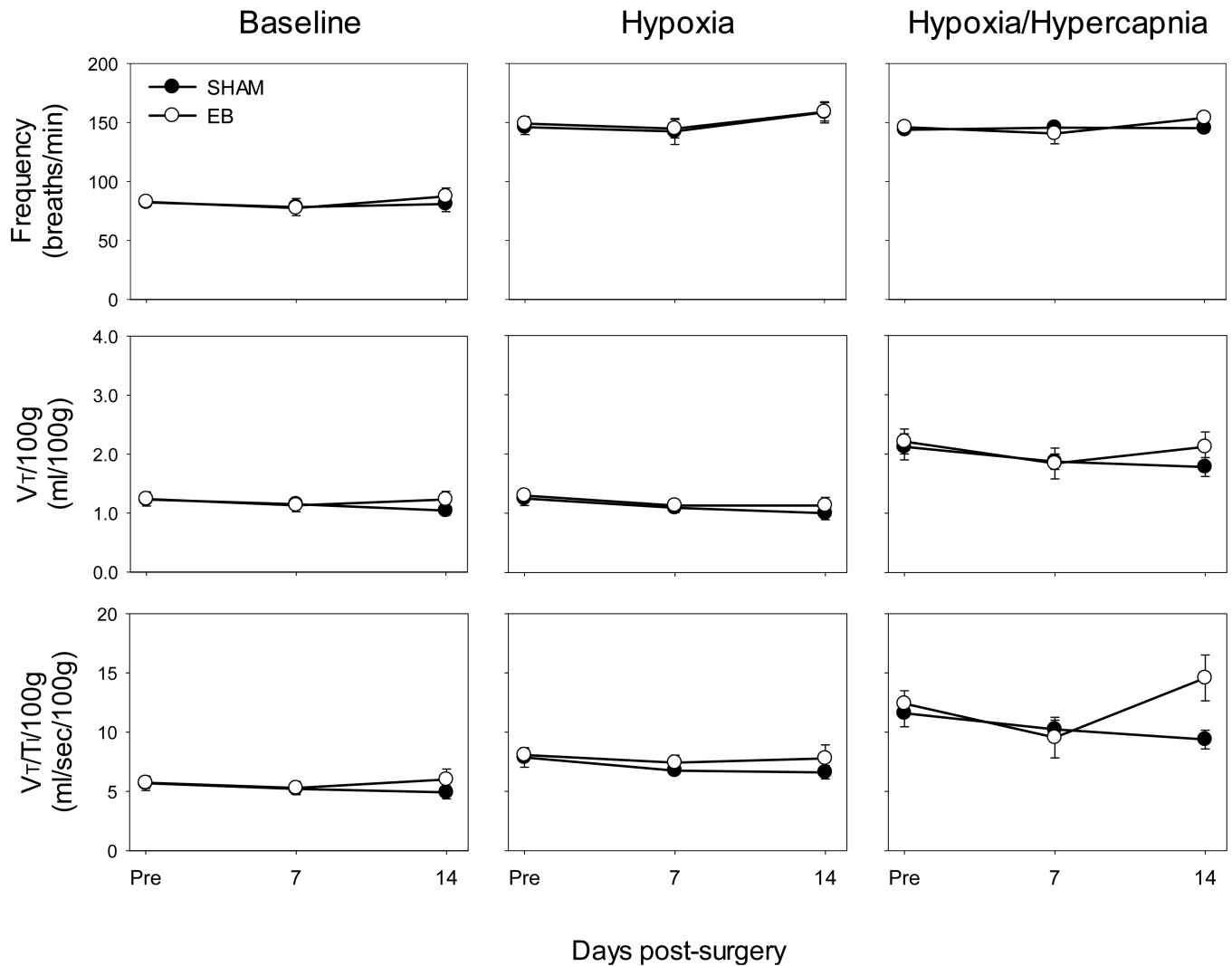
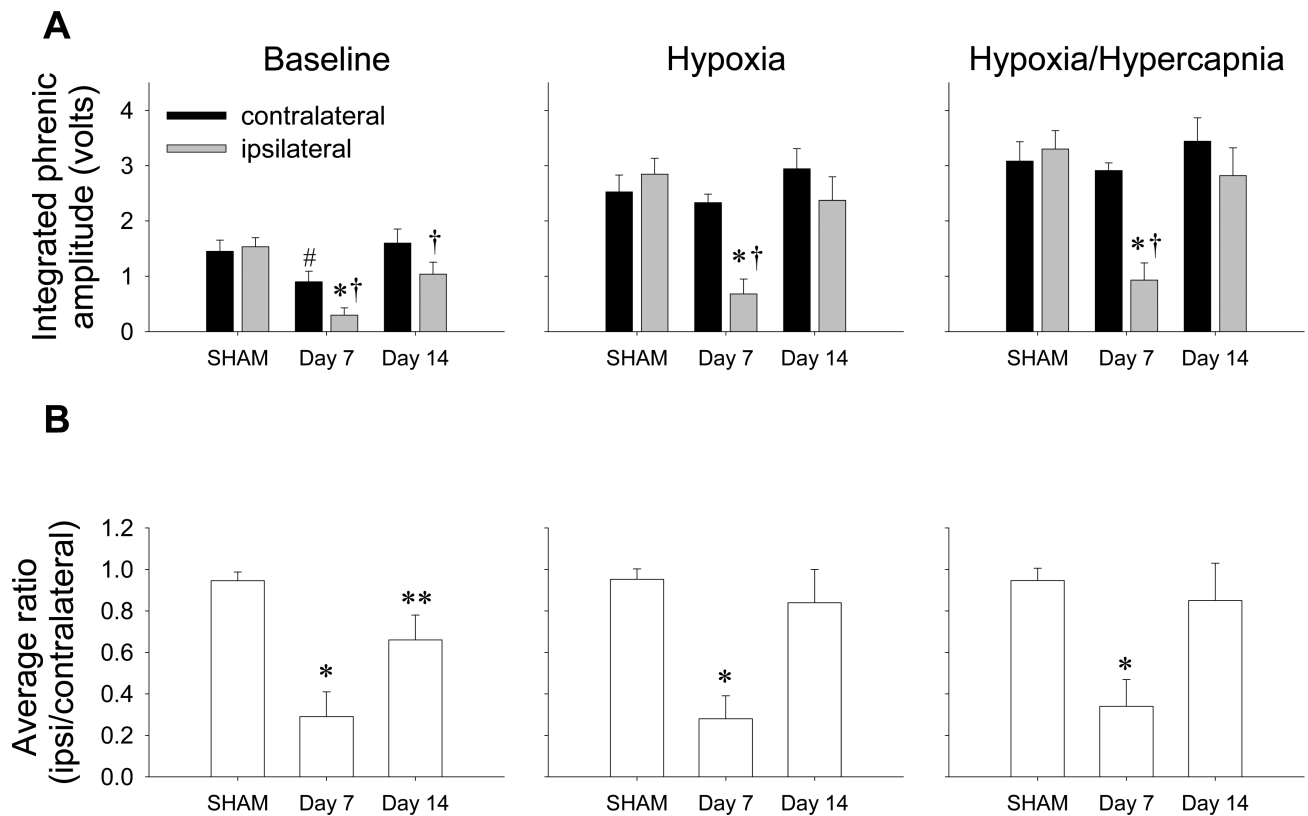


Figure 2. Baseline ventilation (normocapnia) and hypoxic ($F_{I}O_2 = 11\%$) or maximal ($F_{I}CO_2 = 7\%$, $F_{I}O_2 = 11\%$) ventilatory responses in SHAM-injected (closed circles, ●) or EB-injected rats (open circles, ○) pre-injection, 7, and 14 days post-injection. At baseline, in hypoxia, or at maximal chemosensory stimulation, there were no significant differences in frequency, V_T , and V_T/T_I at any time point between SHAM and EB-injected groups (all $P > 0.05$; two-way ANOVA).

**Figure 3.**

Integrated phrenic nerve amplitude (black bars = contralateral phrenic nerve, gray bars = ipsilateral phrenic nerve, **A**) and average ipsi- to contralateral voltage ratios (**B**) in SHAM-injected (all time points combined) or EB-injected rats at 7 and 14 days post-injection at baseline (left panel), hypoxia ($F_{I}O_2 = 11\%$, middle panel) and maximal stimulation ($F_{I}O_2 = 11\%$, $P_{ETCO_2} = 40$ torr above baseline, right panel). (**A**) Baseline ipsilateral phrenic nerve amplitude 7 days post-EB was significantly lower than the ipsilateral amplitude of the SHAM rats and 14 days post-EB ($P < 0.01$ and $P = 0.02$, respectively). Ipsilateral nerve amplitudes at both 7 and 14 days post-EB were significantly lower than the amplitudes of their corresponding contralateral nerves at both times (7 days: $P = 0.01$, 14 days: $P < 0.01$). Contralateral phrenic nerve amplitude 7 days post-EB was also significantly lower than the contralateral amplitude of 14 days post-EB ($P = 0.03$) and was significantly higher than the ipsilateral side ($P = 0.06$). With chemosensory stimulation (hypoxia, hypoxia/hypercapnia), ipsilateral phrenic nerve amplitude 7 days post-EB was significantly lower versus ipsilateral amplitude in SHAM rats (hypoxia, hypoxia/hypercapnia: both $P < 0.001$) and 14 days post-EB (hypoxia, hypoxia/hypercapnia: $P < 0.01$). Further, the ipsilateral phrenic amplitude 7 days post-EB was significantly lower than the contralateral amplitude at the same time point (hypoxia, hypoxia/hypercapnia: both $P < 0.001$). * $P < 0.05$ versus ipsilateral amplitude of SHAM and 14 days post-EB groups, † $P < 0.05$ versus contralateral amplitude within the same corresponding group, # $P < 0.05$ versus 14 days post-EB contralateral amplitude; two-way RM ANOVA. (**B**) Baseline average ipsi/contra ratios at 7 days post-EB were significantly lower than SHAM rats and 14 days post-EB ($P < 0.001$ and $P = 0.02$, respectively). However, the baseline ratio at day 14 remained significantly lower than SHAM levels ($P = 0.03$). The ratios were significantly lower at 7 days post-EB than in SHAM rats or rats 14 days post-EB in hypoxia ($P < 0.001$, $P < 0.01$, respectively) and hypoxia/hypercapnia ($P < 0.01$, $P = 0.02$, respectively). Thus, EB elicits considerable impairment in phrenic nerve output ipsilateral to

injury, and this impairment recovers, at least with chemosensory stimulation, by 14 days.
*P<0.05 versus SHAM and day 14 post-EB injection rat groups, **P<0.05 versus SHAM group only; one-way ANOVA.

\$watermark-text

\$watermark-text

\$watermark-text

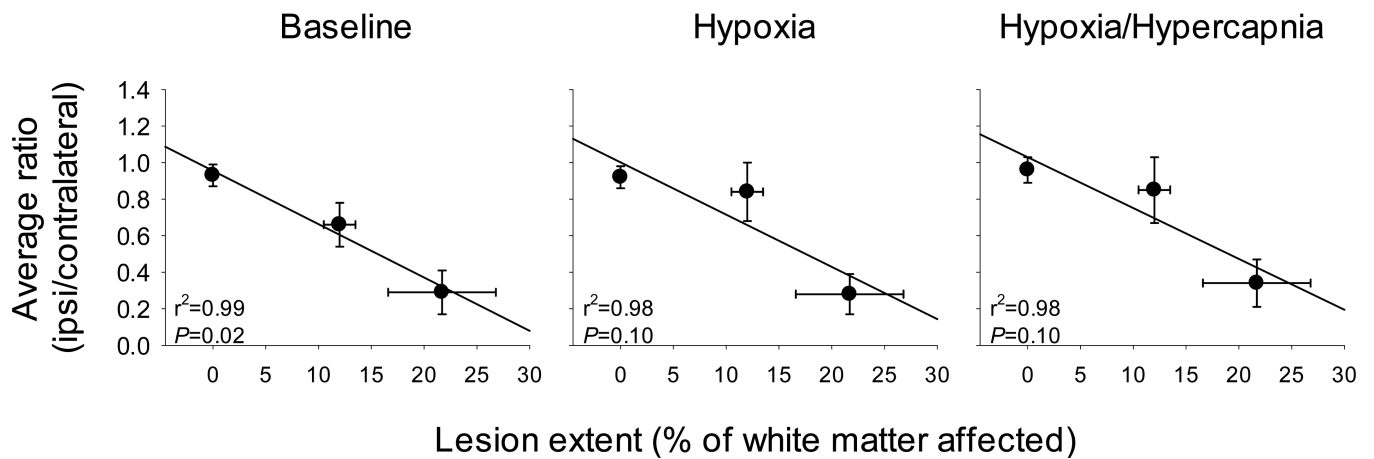


Figure 4.

Average ipsilateral to contralateral phrenic nerve voltages compared to the extent of white matter lesion in SHAM rats and rats 7 and 14 days post-lesioning. At baseline, average ratios were significantly correlated to the lesion extent ($P=0.02$). Although these trends continued in hypoxia and hypoxia/hypercapnia, the regressions were not statistically significant (both $P=0.10$).

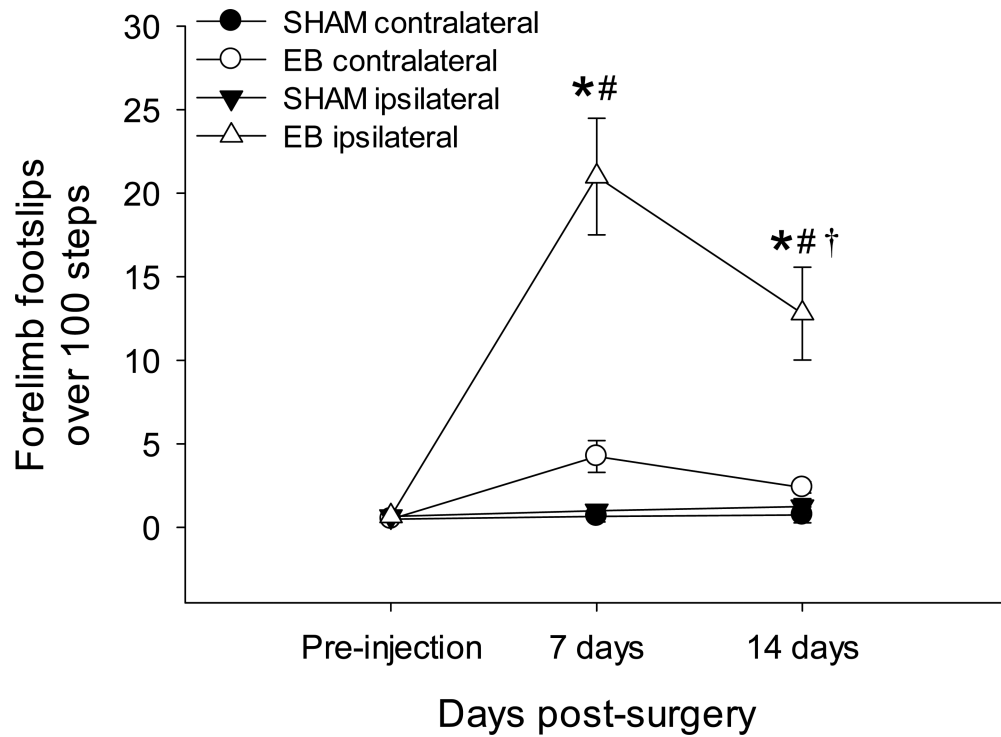


Figure 5.

The average number of foot slips from 100 steps over time. Filled circles indicate foot slips contralateral to the injection site in SHAM rats, filled triangles indicate foot slips ipsilateral to the SHAM injection site, open circles indicate foot slips contralateral to the EB injection, and open triangles indicate foot slips from the ipsilateral limb to the EB injection. SHAM animals showed no differences in function between limbs or over time (all $P > 0.05$). Contralateral limb function of EB-injected rats did not differ from SHAM rats (7 days: $P = 0.24$, 14 days: $P = 0.49$). At 7 and 14 days, the ipsilateral limb of EB rats had significantly more foot slips when compared to pre-injection levels and to the contralateral limb at each time point (all $P < 0.001$). Although the ipsilateral limb of EB-injected rats had less slips at 14 days when compared to the ipsilateral limb at 7 days ($P < 0.001$), the number of foot slips remained significantly higher than pre-injection or SHAM levels at each time point (both $P < 0.001$). * $P < 0.05$ versus contralateral foot slips in EB injected rats and both ipsi- and contralateral foot slips in SHAM rats within the same time point, † $P < 0.05$ versus ipsilateral foot slips 7 days post-EB, # $P < 0.05$ versus pre-injection levels within the same group; two-way ANOVA.